ELSEVIER

Polymer 43 (2002) 4453–4460

polymer

www.elsevier.com/locate/polymer

Synthesis and characterization of ion conducting cellulose esters with PEO side chains

Z. Yue, J.M.G. Cowie*

Department of Chemistry, Heriot-Watt University, Riccarton Campus, Edinburgh EH14 4AS, UK

Received 16 January 2002; received in revised form 11 April 2002; accepted 19 April 2002

Abstract

Cellulose esters with poly(oxyethylene) (PEO) side chains, denoted COE-1 and HPCOE-1A, were prepared through the homogeneous reactions between cellulose or hydroxypropylcellulose and a PEO monocarboxylic acid in the presence of *N*,*N*′-dicyclohexylcarbodiimide and 4-*N*,*N*′-dimethylamino-pyridine. The $LiCF_3SO_3$ complexes of the two polymers were prepared, and the effects of salt concentration on the liquid crystallinity, ionic conductivity and morphology were investigated. It has been found that the two kinds of complexes are both thermotropic liquid crystalline materials and exhibit clearing temperatures, T_c, that increase with increasing salt concentration. The increase in T_c for each system is compensated approximately by a rise in T_g, leaving the liquid crystalline temperature ranges fairly constant. A non-Arrhenius temperature dependence of ionic conductivity is predominant in both systems with the maximum conductivities occurring at [Li]/[O] ≈ 0.07. The environmental scanning electron microscopy reveals a very rough, array-like internal structure for the COE-1 complex at this salt concentration.

Keywords: Cellulose derivatives; Liquid crystallinity; Ionic conductivity

1. Introduction

Since Wright [1,2] reported the ion conducting behaviour of polyethylene oxide (PEO)–alkali salt complexes and Armand et al. [3,4] highlighted the potential of these complexes as polymeric solid electrolytes in high energy density batteries, the research and development of solid polymer electrolytes have attracted world-wide interest. Over the last two decades, a wide range of polymer structures have been explored and great progress has been achieved in improving the level of ionic conductivity. The majority of the polymers being investigated to date are PEO-based copolymers or networks, which is attributed to its high polarity and favourable structural features [5].

Although, it is one of the oldest natural polymers used commercially, the recognition of the liquid crystallinity of cellulose and its derivatives was only made in 1970s [6]. In addition to the chiral nematic phases which are commonly found in many of its derivatives, the nematic and columnar phases have also been reported in some cellulosic systems [7,8]. The formation of liquid crystalline phases in cellulose and its derivatives originates from the inherent semi-rigid nature of the cellulose backbone.

PEO has been incorporated into the cellulose backbone to form ion conducting networks [9–11] with a view to make use of the well-known film-forming aptitude of cellulose. However, the propensity of cellulose derivatives to form liquid crystalline order has not been taken into account. As cellulose is a rich source of liquid crystalline polymers, incorporating PEO side chains onto a cellulose backbone may lead to a new kind of polymer electrolyte where ion conduction takes place in an anisotropic matrix.

In this paper, we report the preparation of two cellulose esters with PEO side chains (COE-1 and HPCOE-1A), and the properties of their $LiCF_3SO_3$ complexes. The well-defined structures of the derivatives enable us to investigate the effect of salt concentration on the liquid crystalline properties, and to find out if there is any correlation between the liquid crystallinity and the ionic conductivities of these complexes. In addition, the effect of adding salt on the morphology of COE-1 was also examined.

* Corresponding author. Tel.: +44-131-451-3106; fax: +44-131-451-3180.

E-mail address: j.m.g.cowie@hw.ac.uk (J.M.G. Cowie).

0032-3861/01/$ - see front matter
PII: S0032-3861(02)00284-7

2. Experimental

2.1. Materials

Cellulose acetate (acetyl content 39.8 wt%, $M_n = 30,000$ g/mol), hydroxypropylcellulose ($M_w = 8000$ g/mol) (HPC), poly[(ethylene glycol)methyl ether] ($M_n = 350$ g/mol) (PEG-350), LiCl, anhydrous *N*,*N*′-dimethylacetamide (DMAc), *N*,*N*′-dicyclohexylcarbodiimide (DCC), 4-[*N*,*N*′-dimethylamino-]pyridine (DMAP), and lithium triflate ($LiCF_3SO_3$) were obtained from Aldrich and used without further purification. Chromium (VI) oxide (CrO_3) was used directly as purchased from Lancaster. The molar substitution of HPC was 3.4, determined by ^{1}H NMR spectroscopy recorded in $CDCl_3$.

2.2. Preparation of cellulose solution

Low molecular weight cellulose was prepared via the hydrolysis of the cellulose acetate. To do so, cellulose acetate (50 g) was stirred in NaOH (50 g) solution in methanol (2 l) for 4 h at room temperature, and the solution was then neutralized with a mixture of glacial acetic acid and water (1:1). The cellulose was collected by filtration and washed with water and methanol several times before being dried in vacuo overnight at 353 K. Complete deacetylation was confirmed by the disappearance of the carbonyl peak in the corresponding IR spectrum.

A 4.6 wt% cellulose solution in 9 wt% LiCl/DMAc was prepared according to a method described by McCormick et al. [12], wherein the dissolution of cellulose was facilitated by a solvent exchange procedure.

2.3. Synthesis of COE-1 and HPCOE-1A

The synthesis of COE-1 and HPCOE-1A is shown in Scheme 1.

2.3.1. Conversion of PEG-350 to PEO-350 monocarboxylic acid (PEO-350 acid)

The oxidation of PEG-350 followed Lele and Kulkarni's procedure [13] but was modified as follows.

In a 1 l beaker, concentrated H_2SO_4 (61 ml) was added in small portions to a stirred solution of CrO_3 (70 g) in deionized water (500 ml) to form a Jones' reagent. The whole process was kept at 283–288 K by using an ice-water bath.

PEG-350 (82 g, 0.23 mol [OH]) was dissolved in 1.5 l acetone, and 400 ml Jones' reagent (containing 0.47 mol CrO_3) was added in several portions. The reaction mixture was stirred at room temperature for 24 h, after which the reaction was quenched by adding 20 ml isopropyl alcohol (free radical scavenger). The solution was then decanted leaving most of the chromium salts at the bottom of the flask, and was concentrated to a viscous liquid, which was extracted subsequently with chloroform (2×300 ml). The combined $CHCl_3$ extracts were washed with water (3×100 ml) and dried over magnesium sulfate. Removal of the solvent yielded a colourless liquid. Yield: 60%; IR (NaCl disc): 3485, 2878, 1744, 1112 cm^{-1}; ^{1}H NMR ($CDCl_3$, δ ppm): 3.1 (s, 3H, $-OCH_3$), 3.3–3.6 (m, 24H, $-OCH_2CH_2-$), 4.0 (s, 2H, $-CH_2CO-$), 10.0 (s, 1H, $-COOH$); ^{13}C NMR ($CDCl_3$, δ ppm): 58.9 ($-OCH_3$), 68.0 ($-CH_2COOH$), 70.0–72.0 ($-OCH_2CH_2-$), 172.5 ($-COOH$).

2.3.2. Determination of the purity of PEO-350 acid [13]

PEO-350 acid (~0.2 g) was dissolved in deionized water (10 ml), and the solution was titrated against 0.0176N KOH solution (normality determined by titration with 0.0210N potassium hydrogen phthalate solution) with phenolphthalein as an indicator. The purity of PEO-350 acid was about 92–96%, as calculated using the following formula:

$$\text{Acid purity (\%)} = 36.4 \times 0.0176 \times (\text{ml KOH required})/\text{weight of sample (g)}.$$

2.3.3. Esterification of cellulose

A 4.6 wt% cellulose solution (12.4 g, 11 mmol [OH]) was stirred in a 100 ml flask, to which was added a solution of DCC (6.6 g, 32 mmol) and DMAP (0.4 g, 3 mmol) in DMAC (20 ml). PEO-350 acid (13.0 g, 36 mmol), diluted with 25 ml of DMAc, was added dropwise over a period of half-an-hour, and the reaction mixture was then heated up to 333 K with stirring for 48 h under nitrogen. Two millilitres of water was added, and the mixture was stirred for another half-an-hour. The white solid was removed by filtration, and the filtrate was poured into diethyl ether. The crude product was dissolved in toluene (300 ml), and after removing the impurities by filtration, the solution was concentrated and precipitated into diethyl ether to yield a viscous liquid. It was purified by another dissolution–precipitation, then dissolved in toluene (300 ml), and the solution was extracted with silica gel to remove any residual polar impurities, concentrated and precipitated into diethyl ether. The product was dried to constant weight in vacuo at RT. IR (NaCl disc): 2873, 1769, 1120 cm^{-1}; ^{1}H NMR ($CDCl_3$, δ ppm): 3.4 (s, $-OCH_3$), 3.5–5.2 (m, oxyethylene chain protons and cellulose backbone protons).

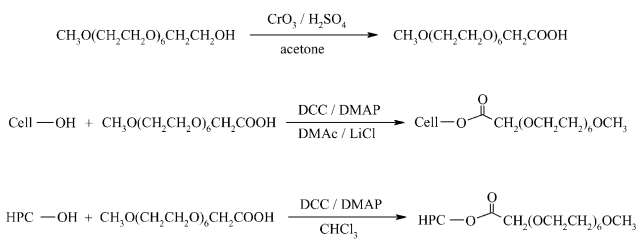

Scheme 1. The synthesis of COE-1 and HPCOE-1A.

2.3.4. Determination of the degree of substitution of COE-1 [14]

COE-1 (~0.3 g) was dissolved in acetone (15 ml) in a 250 ml Erlenmeyer flask. An Erlenmeyer flask with 15 ml acetone was used as blank. Five millilitres of 1 M NaOH solution was added to the two flasks, respectively, and the solutions were stirred overnight at room temperature. The excess of base was then back titrated by 0.181 M HCl with phenolphthalein as an indicator. The procedure was repeated at least twice, and the DS of COE-1 was 2.2, as calculated according to the following formula

$$\mathrm{DS} = \frac{162 \times (V_0 - V_1) \times 0.181 \times 10^{-3}}{W_0 - (V_0 - V_1) \times 0.181 \times 10^{-3} \times (M_{\mathrm{acid}} - 17)}$$

where V_0 and V_1 are the volumes of HCl solution for the blank and the sample; W_0 is the sample weight and M_{acid} is the molecular weight of PEO-350 acid.

2.3.5. Esterification of HPC

HPCOE-1A was prepared and purified using a procedure similar as used for COE-1. The DS value of HPCOE-1A was 3.0, determined by means of ^{1}H NMR spectroscopy. ^{1}H NMR ($CDCl_3$, δ ppm): 1.0–1.4 (d, $-CH-CH_3$), 3.0–5.3 (m, all the other protons).

2.4. Preparation of polymer complexes

Two ranges of $LiCF_3SO_3$ complexes of COE-1 and HPCOE-1A were prepared, respectively, by dissolving appropriate proportions of $LiCF_3SO_3$ and polymer in anhydrous acetonitrile. The solvent was allowed to evaporate slowly under nitrogen and the complexes were dried under vacuum. The concentration of salt in a complex is recorded as the molar ratio of lithium ions to the oxygens in the polymer chain excluding carbonyl oxygens, [Li]/[O]. The oxygens include those in PEO side chains as well as those in the cellulose backbone, although the latter might play a minor role in the ion coordinations.

2.5. Characterization

IR spectra were recorded on a Perkin Elmer RX FT-IR spectrophotometer, and ^{1}H/^{13}C NMR spectra were recorded on a Bruker AC-200 instrument.

Thermal analysis of the derivatives and their complexes was performed by differential scanning calorimetry (DSC) on a DSC 2010 TA instrument at a heating rate of 10 K min^{-1} in a nitrogen atmosphere. The liquid crystalline phases were examined using an Olympus BH-2 polarized light microscope equipped with a Linkam PR600 hot stage, and the clearing temperatures were determined also at a heating rate of 10 K min^{-1}.

Ionic conductivities were measured using a Digital conductivity meter PTI-18 at 1 kHz and the temperatures were controlled by a Haake thermostat bath. The samples were allowed to equilibrate for 1 h at each measuring temperature before the measurement was recorded.

The internal surface morphologies of COE-1 and its complex with [Li]/[O] = 0.07 were examined in a Philips XL30 environmental scanning electron microscope (ESEM) using a Cryo-Stage in high vacuum mode. The Cryo-Stage is an Oxford Instrument CT1500, and an accelerating voltage of 20 kV was used. The samples were placed on PTFE plates and allowed to equilibrate overnight in a desiccator prior to the measurements; the PTFE plates with samples on them were then dipped into liquid nitrogen so that the samples were easily removed without being deformed. The samples were then immediately frozen at 83 K before being transferred under vacuum to the Cryo preparation chamber, where they were fractured in a direction perpendicular to the surface at a temperature below 113 K. The fracture surfaces were gold sputter coated and examined at 93–103 K.

3. Results and discussion

3.1. Synthesis

Cellulose esters are generally synthesized employing an acid anhydride with a catalyst or an acid chloride in the presence of a tertiary base. However, in this work, a more efficient approach is needed as the conventional methods failed to yield a high degree substitution, probably due to the low reactivity of PEO-350 acid anhydride or PEO-350 acid chloride [15].

DCC is a very useful condensation reagent in the coupling of amines and carboxylic acids in peptide and protein chemistry [16]. It has also proven to be an efficient agent in the acylation of an alcohol, if combined with a dialkylaminopyridine [17,18]. Samaranayake and Glasser [19] reported the acylation of cellulose using DCC/4-pyrrolidinopyridine (PP) for the first time, and later Zhang and McCormick [20] reported the preparation of unsaturated cellulose esters using DCC/PP or DCC/DMAP. Although both groups targeted a low DS, a cellulose hexanoate with a DS value as high as 2.5 was also reported. The novel acylation route was attempted in the preparation of COE-1 and HPCOE-1A by treating cellulose or HPC with PEO-350 acid in the presence of DCC/DMAP, and proved to be successful as both products were highly substituted. It may therefore be concluded that this approach is very efficient for the preparation of highly substituted cellulose esters especially those with long side chains. It is noteworthy that the reaction conditions described here may not be the best as no optimization of the esterification was carried out.

3.2. Thermal properties

COE-1 and HPCOE-1A are highly viscous liquids at

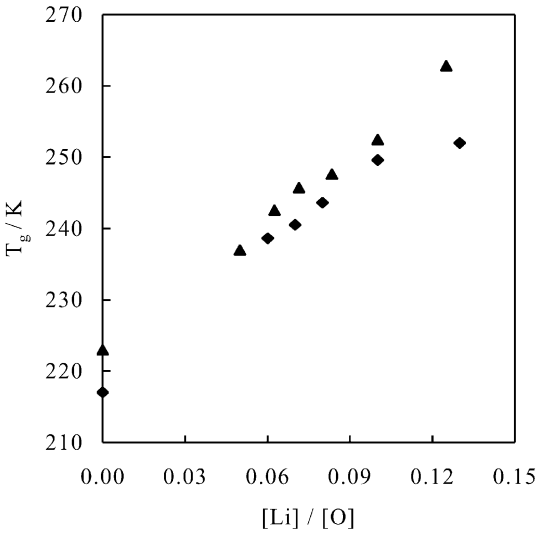

Fig. 1. Variation of the glass transition temperatures (T_g) with the [Li]/[O] ratio for the $LiCF_3SO_3$ complexes of COE-1 (▲) and HPCOE-1A (◆).

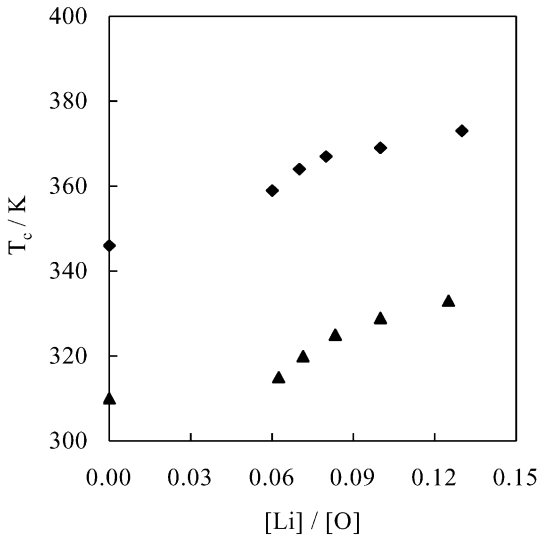

Fig. 2. Variation of the clearing temperatures (T_c) with the [Li]/[O] ratio for the $LiCF_3SO_3$ complexes of COE-1 (▲) and HPCOE-1A (◆).

room temperature, and their DSC thermograms only revealed glass transitions at 223 and 217 K, respectively. The lower T_g of HPCOE-1A may be attributed to its higher DS value and the presence of isopropyl side chains that actually increases the side chain length. As shown in Fig. 1, the T_g values for the $LiCF_3SO_3$ complexes of COE-1 and HPCOE-1A both increase significantly with increasing [Li]/[O] ratio, reflecting a decrease in polymer chain mobility. This is due to the formation of intra- and inter-molecular transient crosslinks resulting from the coordinations between the cations and ether oxygens [21].

COE-1 displays very weak birefringence under a polarized microscope at room temperature, by contrast, its $LiCF_3SO_3$ complexes are more intensely birefringent, exhibiting sanded textures. The liquid crystalline phases formed by the polymer and its complexes may be nematic or chiral nematic, but as there was no feature texture observed, the unambiguous phase assignment could not be made. The COE-1 complexes exhibit a very broad clearing temperature range, and the clearing temperature, T_c, was taken as the temperature when the sample became completely isotropic. Fig. 2 shows that the T_c values for the COE-1 complexes are higher than that of the salt-free polymer and increase progressively with increasing salt concentration. This indicates that the liquid crystalline phases formed by the complexes are more stable at higher temperatures than that formed by the undoped polymer.

In this work, the side chain length of COE-1 is restricted to about six ethylene oxide units (1 unit was oxidized to the carbonyl form) so that no side chain crystallization occurs. The side chains are highly flexible and their conformations tend to be random coils. When the lithium salt is added, the driving force for optimal coordinations between cation and ether oxygen 'pushes' PEO to adopt a helical structure which maximizes the number of coordinating sites [22]. In doing so, the adopted helical structure is stabilized by the coordinations, and consequently the chains become more rigid. The stiffening effect is associated with the ion–dipole interactions between cations and oxygens, and becomes more pronounced as more salt is added. In addition, the accommodation of salt in the polymer chains gives rise to strong intra- and inter-molecular coulombic interactions. All the factors can contribute to a rise in T_c with increasing salt concentration. However, as the T_g of the complexes is increased at the same time, the LC temperature ranges, (T_c–T_g), do not vary too much (within 10 K) within the salt content range used, and are slightly smaller than that of the pure polymer, as shown in Fig. 3.

The rise in T_c induced by adding salt has also been reported in some other systems including the polymers comprising PEO-based backbones with long alkyl side chains [23] or mesogenic side chains [24], and mesogenic

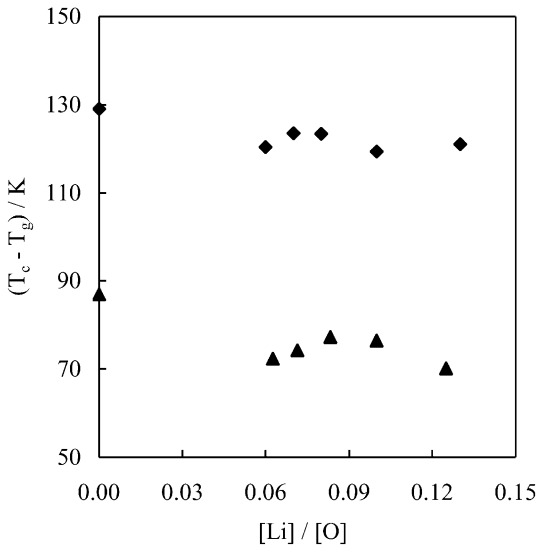

Fig. 3. Variation of the (T_c–T_g) values with the [Li]/[O] ratio for the $LiCF_3SO_3$ complexes of COE-1 (▲) and HPCOE-1A (◆).

dimers containing oxyethylene moieties [25]. All the results demonstrated a significant effect of salt on the mesomorphic behaviour of a liquid crystalline polymer electrolyte. However, the isotropization temperature reflects only one aspect of a liquid crystalline phase. Imrie et al. [26] reported the increasing suppression of T_c endotherms at high salt concentrations for the systems containing mesogenic side chains, which hinted at the tendency towards amorphicity. Since the COE-1 complexes did not show any peak corresponding to isotropization in the DSC traces, the investigation of the salt effect on the liquid crystallinity was limited only to this step–examination of the T_c change.

HPCOE-1A is a thermotropic liquid crystal, and Fig. 4 shows its banded texture induced by shear, which is commonly found in nematic and chiral nematic liquid crystalline polymers [27]. The high birefringence and wider LC range (T_c–T_g) of HPCOE-1A (Fig. 3) are in sharp contrast to those of COE-1. It seems that the isopropyl side chains of HPC favour the formation of a thermotropic mesophase. This point is also reflected in the fact that there is a wide range of thermotropic HPC derivatives compared with the limited number of thermotropic cellulose derivatives. However, comparison between COE-1 and HPCOE-1A should be made cautiously as the two derivatives differ in DS and molecular weight.

As with the COE-1 complexes, the HPCOE-1A complexes are also anisotropic at room temperature, displaying the sanded textures or banded textures if shear is applied. Again since HPCOE-1A and its complexes do not show any characteristic cholesteric texture, it could only be concluded that the mesophases formed by them are nematic or chiral nematic. Fig. 2 also shows that the T_c values for the HPCOE-1A complexes increase with increasing salt concentration. The significant increase in T_c is approximately compensated by a rise in T_g, leaving the LC ranges fairly constant within the salt concentration range being investigated, as shown in Fig. 3. It is also shown in Fig. 3 that the LC ranges for the HPCOE-1A complexes are much wider compared with those of the COE-1 complexes, suggesting that the liquid crystalline phases formed by the former have higher thermal stability.

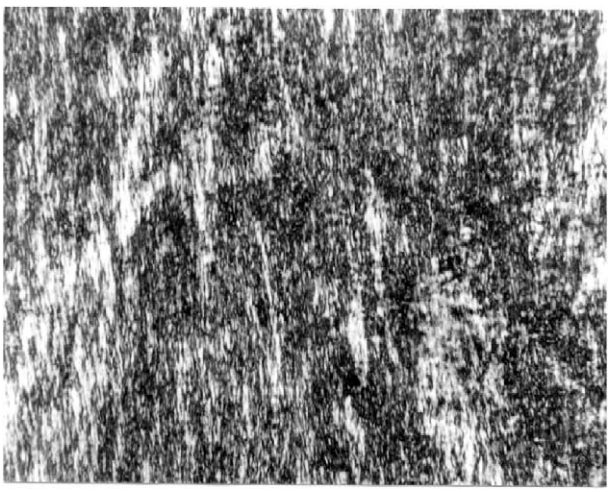

Fig. 4. Banded texture of HPCOE-1A at room temperature.

3.3. Ionic conductivity

The ionic conductivities of the COE-1 complexes with the [Li]/[O] ratios varying from 0.05 to 0.13 were measured over a temperature range of 296–383 K. The conductivities range from $\sim 10^{-6}$ S cm^{-1} at ambient temperatures to $\sim 10^{-4}$ S cm^{-1} at 370 K, which are not exceptionally high when compared with general amorphous PEO-based polymer electrolytes [28]. High ambient conductivities of the order of 10^{-5}–10^{-4} S cm^{-1} have been reported in some PEO-based systems containing highly flexible polymer backbones [29], and the COE-1 complexes are about 1–2 orders of magnitude lower than that. This might be due to the semi-rigid backbone of cellulose, hindering the motion of ions.

Fig. 5 shows the non-Arrhenius plots of log conductivity against ($1/T$) of the COE-1 complexes, and the data were fitted well by the Vogel–Tammann–Fulcher equation [30–32]

$$\sigma = \sigma_0 \exp[-B/(T - T_0)] \quad (1)$$

where constant B can be related to the thermodynamic parameters which characterize the free volume [33], and T_0 is a constant value below T_g. The VTF behaviour observed in the systems indicates that the segmental motion of the polymer chains plays an important role in the ion conducting process, which is a common feature in solid

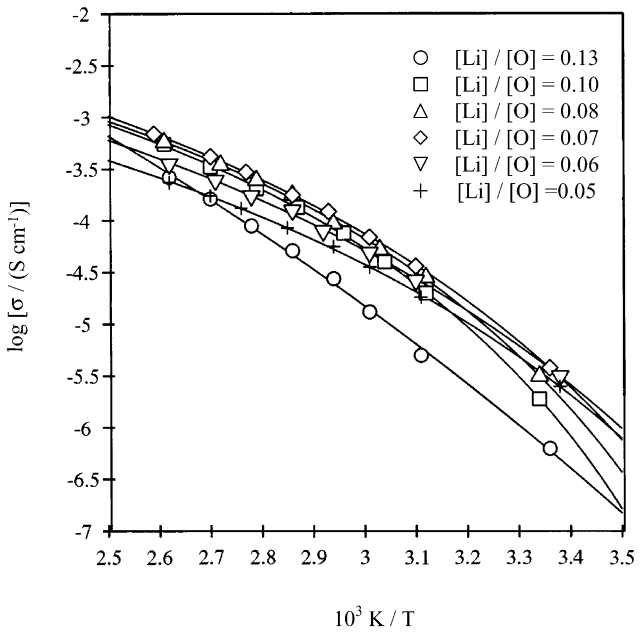

Fig. 5. Plots of $\log \sigma - T^{-1}$ for the $LiCF_3SO_3$ complexes of COE-1 showing the different [Li]/[O] ratios from 0.05 to 0.13. Data were curve fitted using the VTF equation.

polymer electrolytes where the ion transport is assisted by the local relaxation of the polymer chains.

It can be observed in Fig. 5 that there is no apparent kink in the log $\sigma - T^{-1}$ plots at the clearing temperatures of these complexes. Hubbard et al. [34] reported significant changes in the log $\sigma - (1/T)$ plots corresponding to the transition from liquid crystalline phase to isotropic phase for the systems containing mesogenic groups in the main chains. Such a response was also reported in the log $\sigma - T^{-1}$ plots for the systems containing mesogenic side chains [26], but became weaker. It might therefore be deduced that the change associated with the isotropization in the log $\sigma - T^{-1}$ plot depends on the structure of the individual liquid crystalline system including the polymer and the salt, and the liquid crystalline properties. In contrast to the smectic phases formed by the earlier mentioned systems [26,34] where the conductivity response corresponding to isotropization was evident in the log $\sigma - T^{-1}$ plots, the liquid crystalline phases of the COE-1 complexes were nematic or chiral nematic. The thermal transition from a nematic phase to isotropic phase is generally very weak, as for the COE-1 complexes, there is no discernible endothermic peak associated with the isotropization in the DSC scans, indicating that the difference in the molecular ordering between the two states is very small. Therefore, for the systems studied here the corresponding change in conductivity might be too weak to be reflected in the log $\sigma - T^{-1}$ plots.

Fig. 6 shows the concentration dependence of ionic conductivity of the COE-1 complexes, in which the maximum conductivities occur at [Li]/[O] $\approx$ 0.07 for all the temperatures being studied. The ionic conductivity of a homogeneous polymer electrolyte is closely related to two important factors, the number of charge carriers, n_i, and the mobility of ion species, μ_i [21]. The charge carriers also include mobile charged aggregates. Adding more salt will inevitably increase the numbers of charge carriers, which is good for promoting conductivity, but this effect will be eventually offset by a reduction in the ion mobility, leading to the occurrence of a maximum at a certain salt concentration. The decrease in the ion mobility is mainly caused by the increasing tendency to form higher, less mobile ion species and a decrease in the polymer chain mobility as being reflected in an increase in T_g. The studies of polymer electrolytes are generally carried out in the range of salt concentration approximately 0.05 (in terms of the [Li]/[O] ratio) or above, where the ion–ion interactions are extensive and ions tend to form ion pairs or other mobile aggregates [35,36]. Increasing salt concentration will lead to the formation of less mobile, higher clusters. In addition, the coordinations between the cations and ether oxygens stiffen the polymer chain and decrease its ability to ionize the salt, which also contributes to a fall in the ionic conductivity.

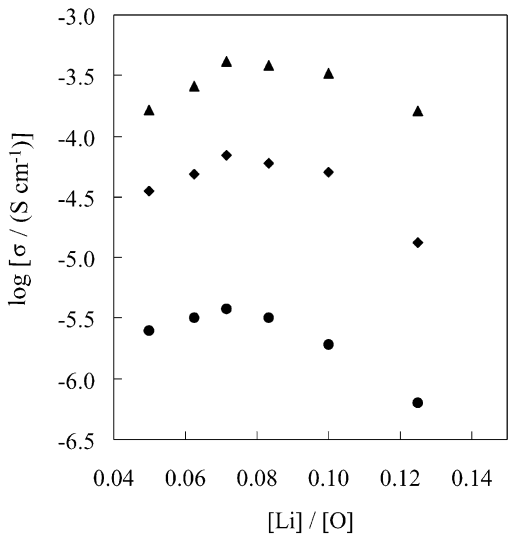

Fig. 6. Isothermal plots of log σ against the [Li]/[O] ratio for the COE-1 $LiCF_3SO_3$ complexes; (●) $T = 297$ K; (◆) $T = 332$ K; (▲) $T = 370$ K.

The ionic conductivities of the HPCOE-1A complexes are of the same order of magnitude as those of the COE-1 complexes, and also display a VTF type temperature dependence (Fig. 7). As with the COE-1 systems, there is no apparent inflection corresponding to the transition from the liquid crystalline phases to isotropic phase in the log $\sigma - T^{-1}$ plots of the HPCOE-1A complexes. This is again probably because such a conductivity response is too weak to be reflected in the log $\sigma - T^{-1}$ plots. Among the systems, the complex with [Li]/[O] $\approx$ 0.07 gives the best range of conductivities for all the temperatures being investigated (Fig. 8).

3.4. Environmental scanning elemental microscopy

In the present polymer–salt systems, the amounts of salt

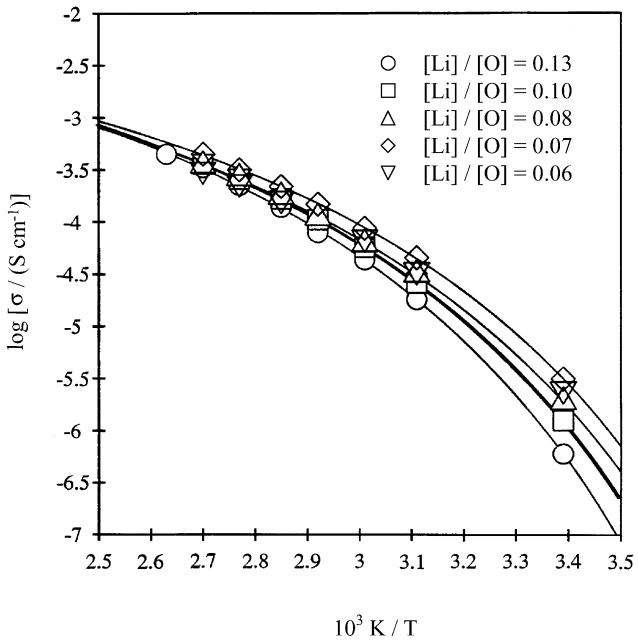

Fig. 7. Plots of log $\sigma - T^{-1}$ for the $LiCF_3SO_3$ complexes of HPCOE-1A showing the different [Li]/[O] ratios from 0.06 to 0.13. Data were curve fitted using the VTF equation.

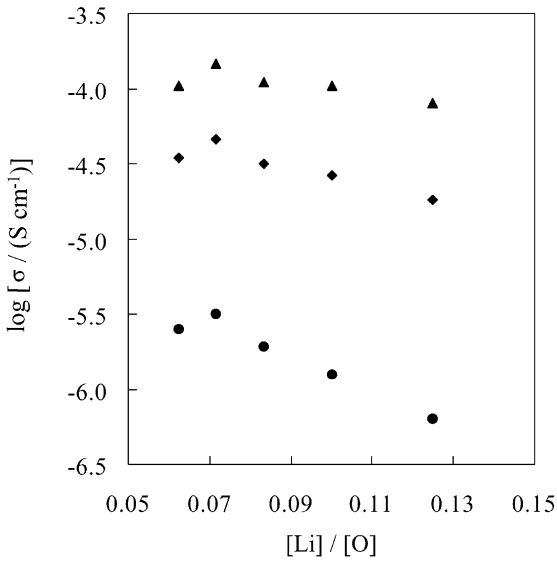

Fig. 8. Isothermal plots of log σ against the [Li]/[O] ratio for the $LiCF_3SO_3$ complexes of HPCOE-1A; (●) $T = 293$ K; (◆) $T = 322$ K; (▲) $T = 342$ K.

employed are significant, for instance, the [Li]/[O] ratios of the COE-1 complexes range from 0.05 to 0.13, corresponding to the weight concentrations of $LiCF_3SO_3$ from 15 to 30%. It is conceivable that adding such significant amounts of salt must cause a pronounced effect in the structure and morphology. For this reason, the freeze fractured surfaces of COE-1 and its complex with [Li]/[O] = 0.07 were examined with ESEM and the micrographs are shown in Fig. 9.

As can be observed, COE-1 shows the existence of some kind of layered structure in its fractured surface, but the layers are not well developed. The internal structure of the COE-1 complex is oriented, displaying array-like arrangements, which are aligned in a direction approximately parallel to the fracture surface. It seems that the arrays are composed of granular-like entities which conglomerate irregularly to form a very rough morphology.

A solid polyether-based electrolyte (except the chemically crosslinked systems) virtually contains a kind of transient crosslinked structure derived from the inherent coordinations between cations and ether oxygens. Given the amount of salt that is generally employed for solid polymer electrolytes, the aggregations of ion species are inevitable [34,35] even in the case of a homogeneous polymer–salt mixture. The COE-1 complex with [Li]/[O] = 0.07 is liquid crystalline at room temperature, and its structure might be described as some sort of ordered alignments of the cellulose backbones with the transient crosslinks occurring in the side chains, accompanied by the existence of regions of ion aggregates. The morphology revealed by the ESEM image of the COE-1 complex tends to support this idea.

4. Conclusions

Cellulose esters with PEO side chains, COE-1

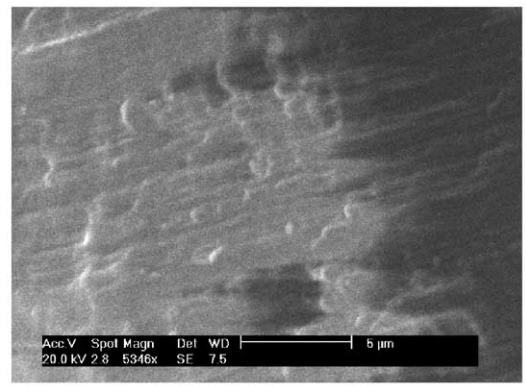

(a)

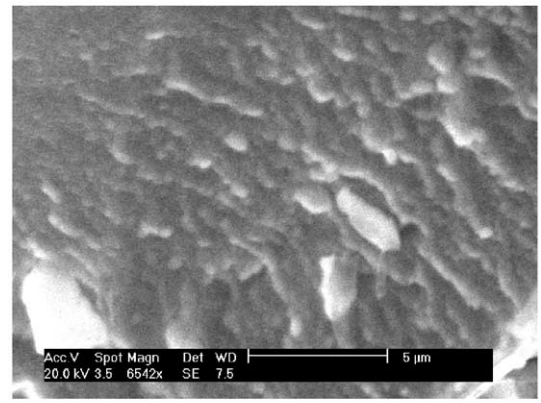

(b)

Fig. 9. Electron micrographs of COE-1 and its $LiCF_3SO_3$ complex (fracture surface morphology); (a) COE-1 and (b) the complex with [Li]/[O] = 0.07.

(DS = 2.2) and HPCOE-1A (DS = 3.0), were synthesized successfully through the homogeneous reactions of cellulose or HPC with PEO-350 acid in the presence of DCC/DMAP.

The two derivatives and their $LiCF_3SO_3$ complexes exhibit thermotropic liquid crystallinity. For both the salted systems, increasing salt concentration leads to an increase not only in T_c but also in T_g, with the LC temperature ranges remaining fairly constant within the salt concentration range used. The liquid crystalline phases formed by HPCOE-1A and its complexes exhibit higher thermal stability when compared with COE-1 and its complexes.

Both the COE-1 complexes and the HPCOE-1A complexes exhibit a non-Arrhenius temperature dependence of conductivity, with the maximum conductivities occurring at [Li]/[O] $\approx$ 0.07 for all the temperatures being studied. No correlation has been found between the liquid crystalline properties and ionic conductivity in both systems.

The ESEM analysis revealed a significant effect of salt on the morphology of COE-1. A question is raised as to whether this rough but ordered morphology is unique to this kind of liquid crystalline network in which the transient crosslinks take place in the side chains and various ion

aggregates are present. To answer this question, further investigation was carried out on another complex system and the results are presented in a later publication [37].

Acknowledgments

Z. Yue thanks the CVCP for an ORS award, the University of Heriot-Watt for a studentship, and API Foils for additional financial support.

References

[1] Fenton DE, Parker JM, Wright PV. Polymer 1973;14:589.
[2] Wright PV. Br Polym J 1975;7:319.
[3] Armand MB, Chabagno JM, Duclot M. Second International Meeting on Solid Electrolytes. St Andrews, Scotland, 1978.
[4] Armand MB, Chabagno JM, Duclot M. In: Vashisha P, Mundy JN, Shenoy GK, editors. Fast ion transport in solids. New York: North Holland; 1979. p. 131–6.
[5] Cowie JMG. Macromol Symp 1995;98:843.
[6] Werbowyj RS, Gray DG. Mol Cryst Liq Cryst (Lett) 1976;34:97.
[7] Yang K-S, Theil MH, Cuculo JA. In: El-Nokaly MA, editor. Polymer association structures. American Chemistry Society Symposium Series, 384; 1989. p. 156.
[8] Yamagishi Y, Fukuda T, Miyamoto T, Yakoh Y, Takashina Y, Watanabe J. Liq Cryst 1991;10(4):467.
[9] Le Nest JF, Gandini A, Xu L, Schoenenberger C. Polym Adv Technol 1993;4:92.
[10] Schoenenberger C, Le Nest JF, Gandini A. Electrochim Acta 1995;40: 2281.
[11] Schoenenberger C, Le Nest JF, Gandini A. In: Kennedy JF, editor. The chemistry and processing of wood and plant fibrous materials. London: Woodhead Publishers; 1995. p. 351.
[12] McCormick CL, Callais PA, Hutchinson Jr BH. Macromolecules 1985;18(12):2394.
[13] Lele BS, Kulkarni MG. J Appl Polym Sci 1998;70:883.
[14] Rusig I, Dedier J, Filliatre C, Godhino MH, Varichon L, Sixou P. J Polym Sci, Part A: Polym Chem 1992;30:895.
[15] Yue Z. PhD thesis, Heriot-Watt University, 2002.
[16] Haslam E. Tetrahedron 1980;30:2409.
[17] Hassner A, Alexanian V. Tetrahedron Lett 1978;46:4475.
[18] Hassner A, Krepski L, Alexanian V. Tetrahedron 1978;34:2069.
[19] Samaranayake G, Glasser WG. Carbohydr Polym 1993;22:1.
[20] Zhang ZB, McCormick CL. J Appl Polym Sci 1997;66:293.
[21] Gray FM. Solid polymer electrolytes fundamentals and technological applications. Weinheim: VCH publisher; 1991. Chapter 5.
[22] Papke BL, Ranter MA, Shriver DF. J Phys Chem Solid 1991;42:493.
[23] Dias FB, Batty SV, Gupta A, Ungar G, Voss JP, Wright PV. Electrochim Acta 1998;43:1217.
[24] McHattie GS, Imrie CT, Ingram MD. Electrochim Acta 1998;43: 1151.
[25] Ohtake T, Takamitsu Y, Ito-Akita K, Kanie K, Yoshizawa M, Mukai T, Ohno H, Kato T. Macromolecules 2000;33:8109.
[26] Imrie CT, Ingram MD, McHattie GS. J Phys Chem 1999;103:4132.
[27] Viney C, Putnam WS. Polymer 1995;36(9):1731.
[28] Meyer WH. Adv Mater 1998;10:439.
[29] Cowie JMG. The encyclopaedia of advanced materials. In: Bloor D, Brook RJ, Flemings MC, Mahajan S, editors. Ionic conductivity of polymers. New York: Pergamon Press; 1994. p. 1195.
[30] Vogel H. Phys Z 1921;22:645.
[31] Tammann VG, Hesse WZ. Anorg Allg Chem 1926;156:245.
[32] Fulcher GS. J Am Chem Soc 1925;8:339.
[33] MacCallum JR, Vincent CA. Polymer electrolyte review I. Amsterdam: Elsevier Science; 1987. Chapter 7.
[34] Hubbard HVStA, Sills SA, Davies GR, McIntyre JE, Ward IM. Electrochim Acta 1998;10–11:1239.
[35] Wright PV. J Mater Chem 1995;5(9):1275.
[36] Gray FM. Solid polymer electrolytes fundamentals and technological applications. Weinheim: VCH publisher; 1991. Chapter 9.
[37] Yue Z, McEwen IJ, Cowie, JMG. J Mater Chem, in press.